Preliminary Results of Exploring the Behaviour of Phyllosilicates When Subject to Thermal Conditions Relevant to Asteroid Ryugu

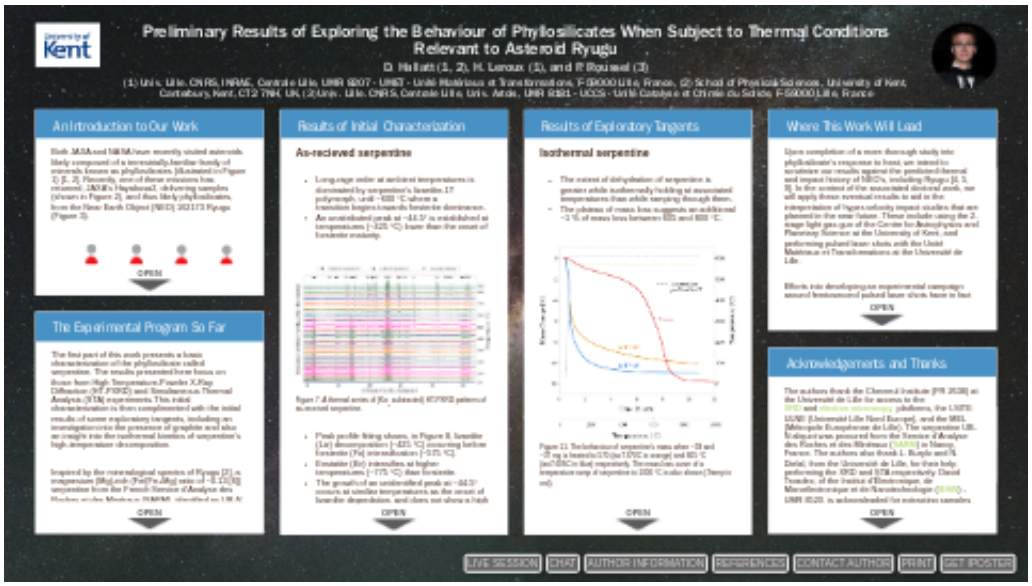

D. Hallatt (1, 2), H. Leroux (1), and P. Roussel (3)

(1) Univ. Lille. CNRS, INRAE, Centrale Lille, UMR 8207 - UMET - Unité Matériaux et Transformations, F-59000 Lille, France, (2) School of Physical Sciences, University of Kent, Canterbury, Kent, CT2 7NH, UK, (3) Univ. Lille. CNRS, Centrale Lille, Univ. Artois, UMR 8181 - UCCS - Unité Catalyse et Chimie du Solide, F-59000 Lille, France

PRESENTED AT:

LPSC 52
Virtual Conference | 03.15–19. 2021

AN INTRODUCTION TO OUR WORK

Both JAXA and NASA have recently visited asteroids likely composed of a terrestrially-familiar family of minerals known as phyllosilicates (illustrated in Figure 1) [1, 2]. Recently, one of these missions has returned, JAXA's Hayabusa2, delivering samples (shown in Figure 2), and thus likely phyllosilicates, from the Near Earth Object (NEO) 162173 Ryugu (Figure 3).

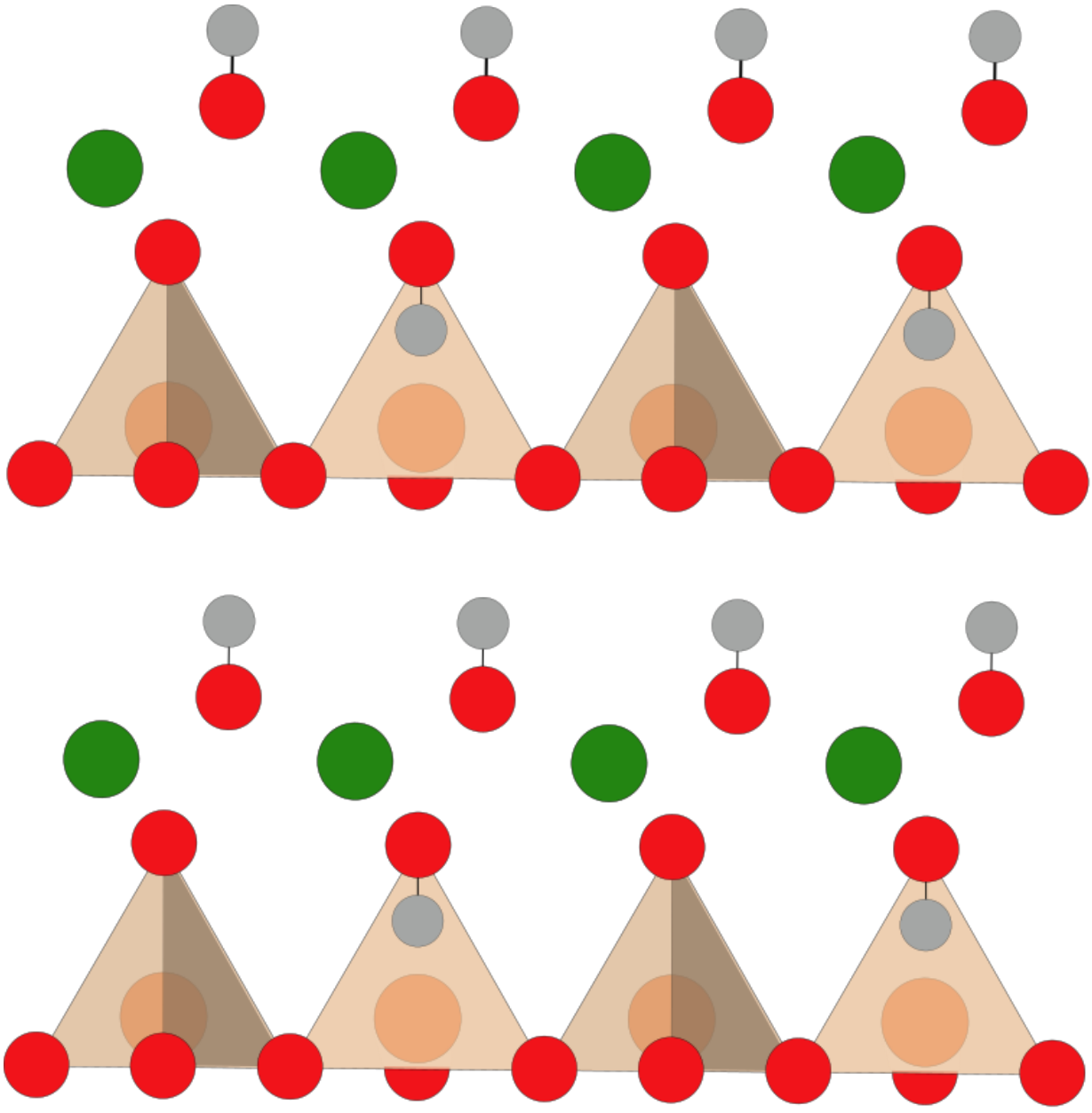

Figure 1: A schematic representation of the basic atomic arrangement in a basic phyllosilicate structure. Key: red = oxygen, orange = silicon, grey = hydrogen, green = metal (magenesium, iron, aluminium, ect.).

Figure 2: One of the sample compartments of the Hayabusa2 mission, holding material collected from asteroid Ryugu. * This image is courtesy of the JAXA Hayabusa2 webpage (https://www.hayabusa2.jaxa.jp/en/topics/20201225_samples/).

Figure 3: The asteroid 162173 Ryugu, as seen from orbit by the Optical Navigation Camera (ONC) onboard the Hayabusa2 spacecraft. * This image was produced from the publically available JAXA Data Archives and Transmission System (*DARTS (https://data.darts.isas.jaxa.jp/pub/hayabusa2/paper/Watanabe_2019/README.html)*) associated with Watanabe, *Science*, 2019.

However, while such small, extraterrestrial bodies represent sources of material from different times and places within the Solar System, the potentially hydrated and organic bearing [3] sheet(phyllo)-silicates are not immune to the conditions plausibly experienced by NEOs. The behaviour of phyllosilicates is therefore not only required to deduce theories about their primitive origins, but can also be exploited to help chronicle their since-storied past, as a translation of those messages from the foreign bodies which they have comprised.

Currently, the most explored interpretations of Ryugu's material state have involved a major component due to thermal annealing (proposed via radiative solar heating) [4, 5]. It is here where we present an early extension of our impact-centric work, which is concerned with eventually informing the thermal role of hypervelocity impacts involving a phyllosilicate-bearing body. Here, we apply our preliminary results from characterizing the thermal behaviour of phyllosilicates, to the proposed domains of heating that Ryugu's material-constituents may have been subject to. This poster intends to act as a setting for demonstrating the earliest results and research questions/directions of a doctoral thesis focused on impact alteration of phyllosilicates on bodies like Ryugu.

THE EXPERIMENTAL PROGRAM SO FAR

The first part of this work presents a basic characterization of the phyllosilicate called serpentine. The results presented here focus on those from High Temperature-Powder X-Ray Diffraction (HT-PXRD) and Simultaneous Thermal Analysis (STA) experiments.This initial characterization is then complimented with the initial results of some exploratory tangents, including an investigation into the presence of graphite and also an insight into the isothermal kinetics of serpentine's high-temperature decomposition.

Inspired by the mineralogical spectra of Ryugu [2], a magnesium (Mg)-rich (Fe/(Fe+Mg) ratio of ~0.13 [6]) serpentine from the French Service d'Analyse des Roches et des Minéraux (SARM), identified as *UB-N*, was chosen to be the first phyllosilicate investigated. We find good agreement with prior reports that, acccording to PXRD, UB-N it is structurally dominated by the lizardite polymorph [7]. Furthermore, our aliquot (shown in Figure 4) has a composition and particle size also similar to those reported: between 1-100 μm and roughly $Ca_{0.05}Mg_{2.6}Fe_{0.4}Al_{0.1}Si_{1.9}O_5(OH)_4$ [6].

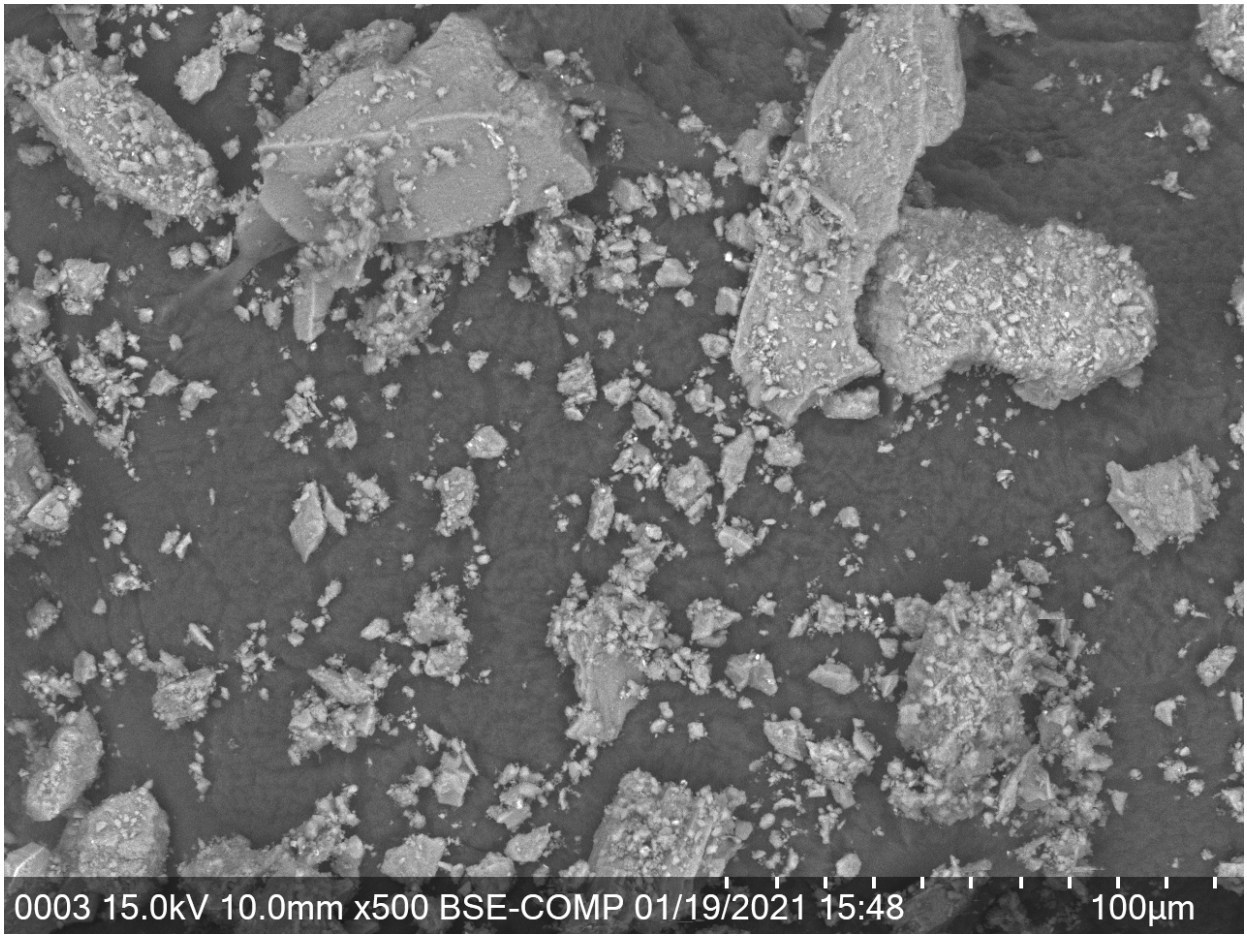

Figure 4. A backscatter electron image of UB-N serpentine, captured using an SEM at the Chevreul Institute, Université de Lille.

All of the HT-PXRD experiments employed a Bruker D8 Advance instrument with a Cu anode (λ = 1.5418 Å), equipped with a LynxeEye XE 1D detector and an Anton Parr XRK 900 reactivity chamber. Operating in Bragg-Brentano geometry, each of the HT-PXRD temperature-ramp scans were collected between 9 and 64° (2θ) every 25°C from 25 °C to 850 °C. Analysis of the HT-PXRD results was performed mainly using the Materials Data (MDI)/International Centre for Diffraction Data - JADE (https://www.icdd.com/mdi-jade/?gclid=Cj0KCQiA7YyCBhD_ARIsALkj54qRkmVZiYwaxTolSmcQn8H0uQ8ZQEfi8LOuYcagTmVtoKbA5jKvKUkaAsgFEALw_wcB) software.

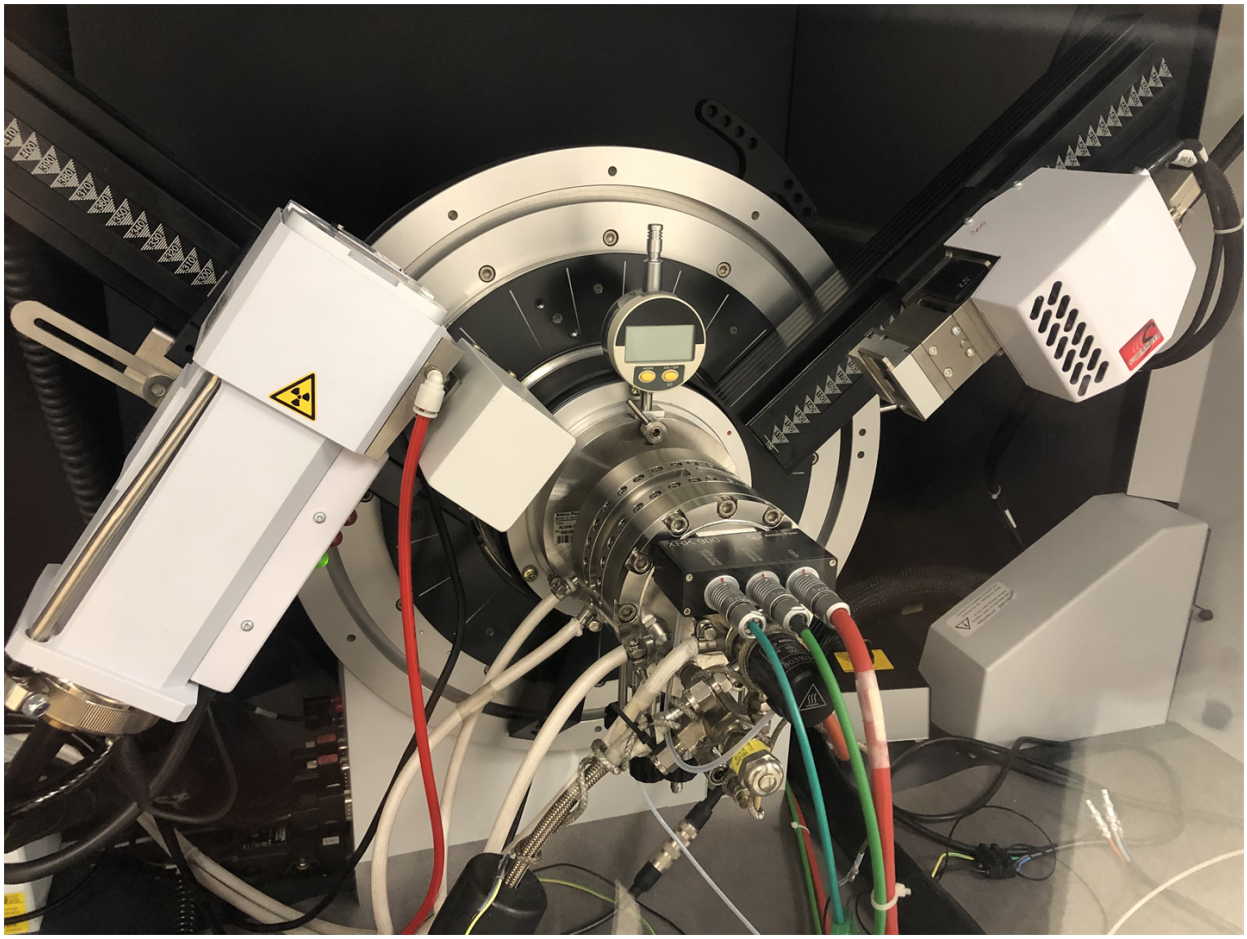

Figure 5. The HT-XRD stetup used at the Chevreul Institute, Université de Lille.

STA was conducted with a Mettler-Toledo TGA/DSC 3+ instrument using an open alumina crucible. In calculating the Differential Thermogravimetric Analysis (DTG) signal, the data was subject to a Savitzky-Golay filter for smoothing. In both the HT-PXRD and STA, a flowing H_2/N_2 (3 vol.%) cover-gas was used for redox control.

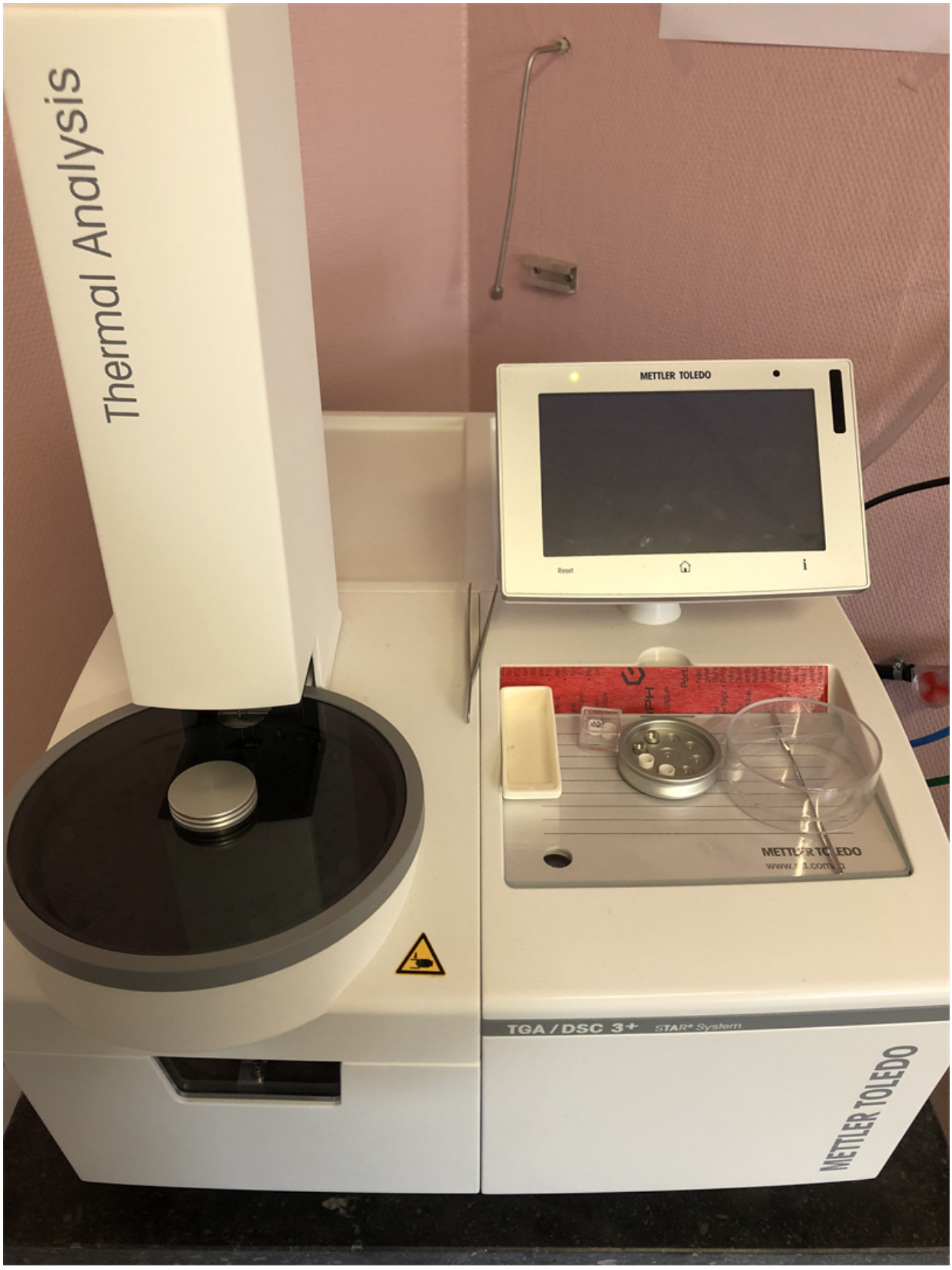

Figure 6. The Mettler-Toledo 3+ instrument used for STA, housed in the Unité de Catalyse et Chimie du Solide at the Université de Lille.

Scanning electron microscopy (SEM) and electron dispersive spectroscopy (EDS) have been also employed, to characterize the sample's morphology and composition respectively. This microscopy work, however, is relatively ongoing and the associated resuts will not be presented here.

RESULTS OF INITIAL CHARACTERIZATION

As-recieved serpentine

- Long-rage order at ambient temperatures is dominated by serpentine's lizardite-1T polymorph, until ~600 °C where a transition begins towards forsterite dominance.
- An unattributed peak at ~44.5° is established at temperatures (~425 °C) lower than the onset of forsterite maturity.

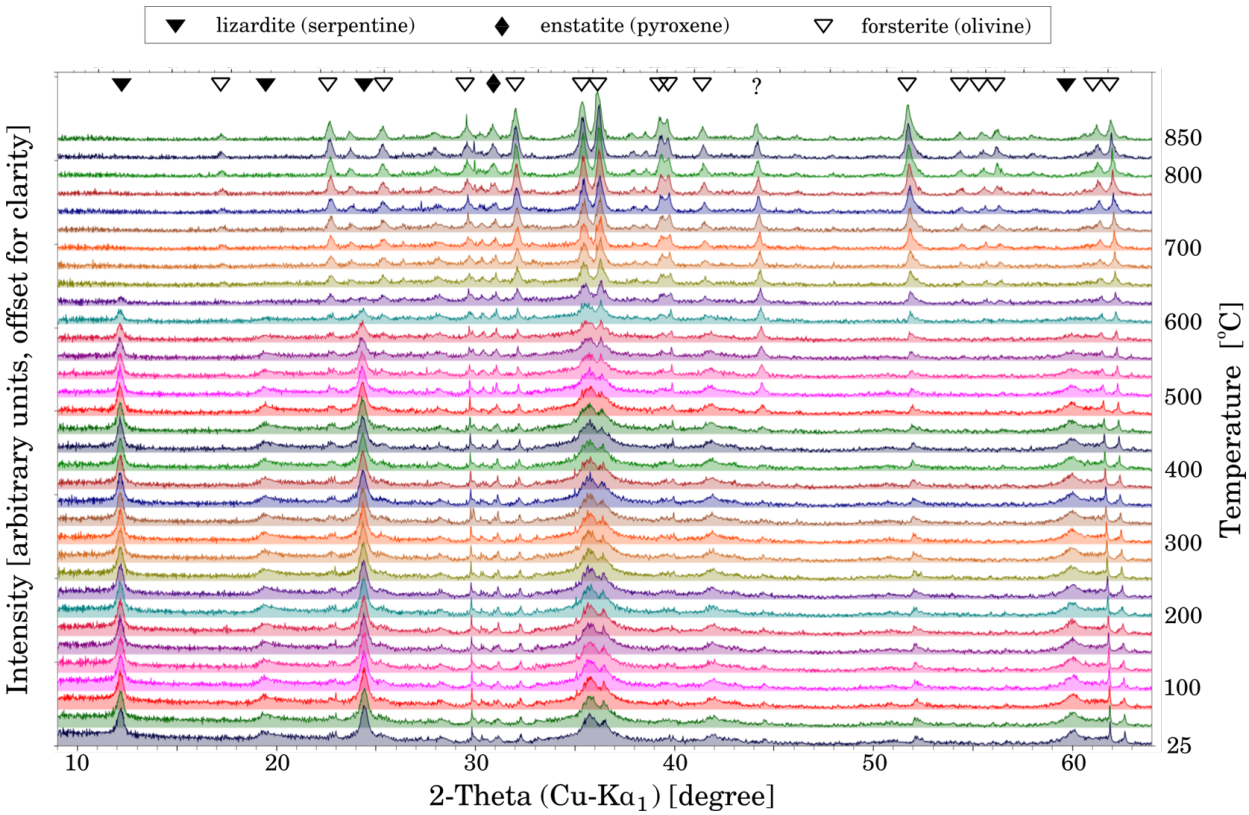

Figure 7. A thermal series of ($K\alpha_1$ subtracted) HT-PXRD patterns of as-received serpentine.

- Peak profile fitting shows, in Figure 8, lizardite (*Liz*) decomposition (~425 °C) occurring before forsterite (*Fo*) intensification (~575 °C).
- Enstatite (*En*) intensifies at higher temperatures (~775 °C) than forsterite.
- The growth of an unidentified peak at ~44.5° occurs at similiar temperatures as the onset of lizardite degredation, and does not show a high temperature spike in intensity like forsterite or enstantite do, instead plateauing at ~500 °C.
- All lizardite peaks (sharp at 17° or broad at 19°) decompose with similar onset and endset temperatures.

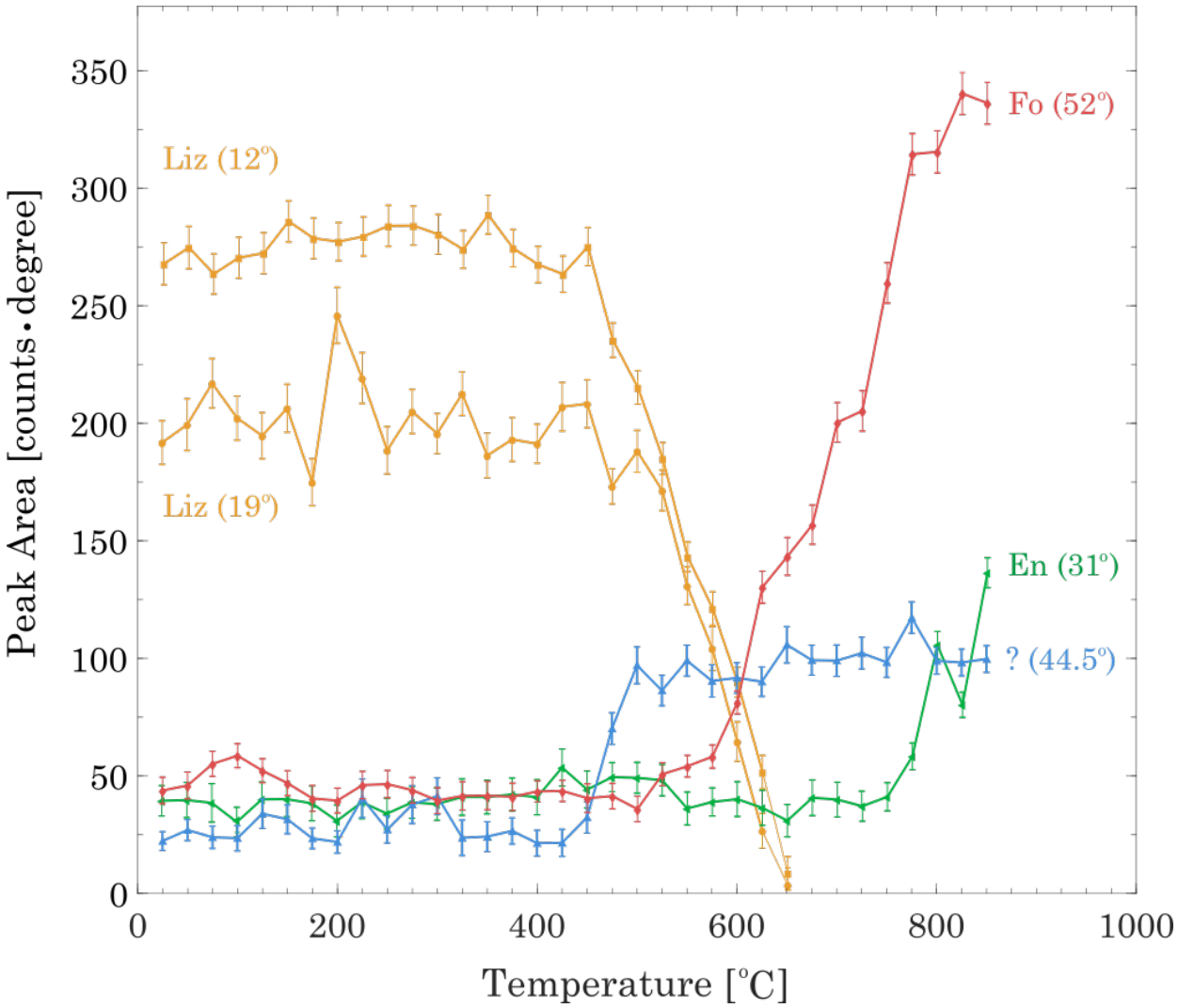

Figure 8. The thermal evolution of particular HT-PXRD peaks' heights from serpentine's thermal series. Using the batch mode of MDI-JADE software, each peak was profile fit with a Pseudo-Voigt peak shape function and a parabolic background to minimize each fit's residual error (all having R<10). Error bars represent ±1σ confidence.

- The peak intensity shown in Figure 9 elucidates a drastic rise and fall in the background signal occuring at temperatures between lizardite and forsterite dominance. Does this suggest a re-crystallization of the high-T phases from an amorphous mid-T?

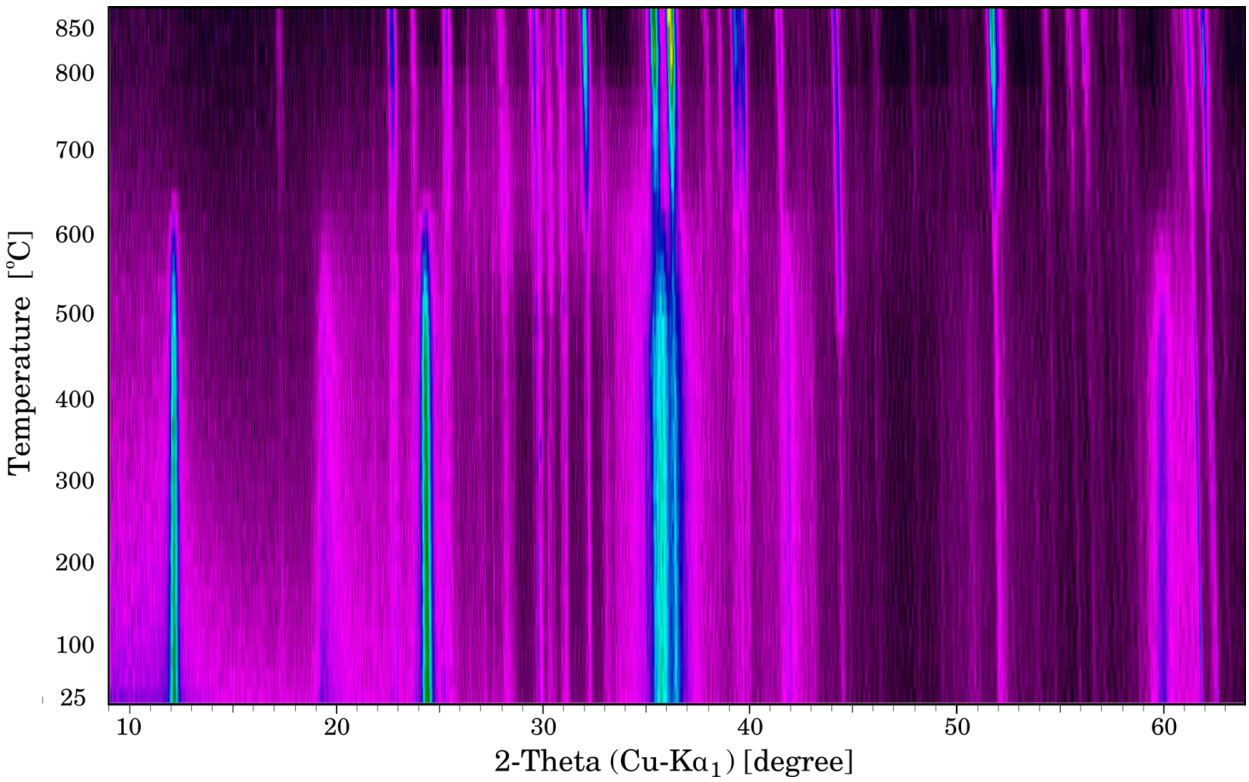

Figure 9. A peak intensity heatmap of serpentine's HT-PXRD thermal series.

- Three distinct regions of mass loss are evident in the DTG signal of Figure 10. The lower and upper events coincide with the onset of lizardite decomposition and forsterite recrystallization respectively.
- The overall mass loss of ~12 %, along with lower and upper mass events (<600 and ~800 °C), agree well with literature [8].
- The intermediate DTG peak occurs at significantly lower temperature than recently reported [8] and coincides with the high-background (amorphous?) region of HT-PXRD scans.

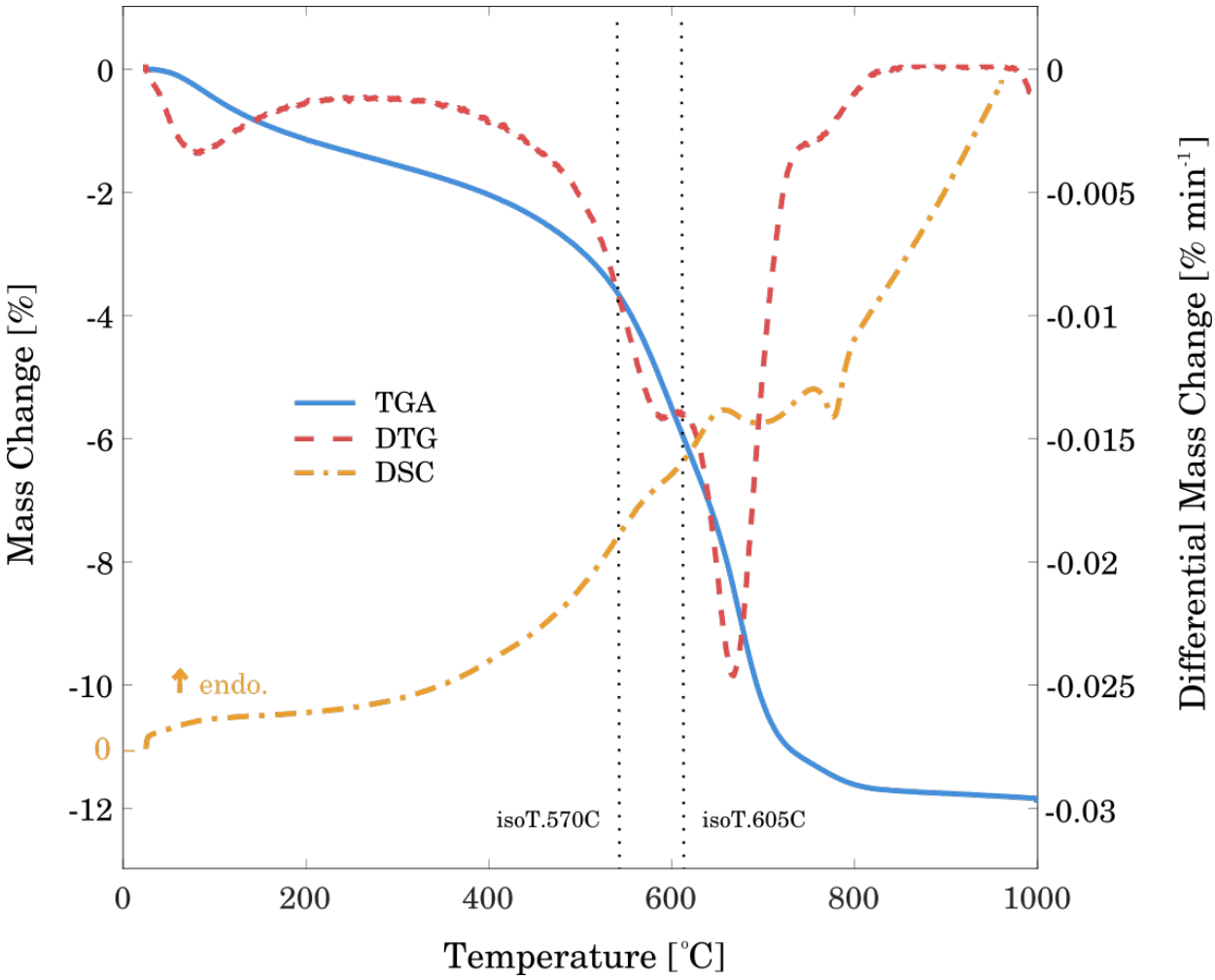

Figure 10. The behaviour of serpentine's mass and thermal energy when ~39 mg is heated to 1000 °C under H_2/N_2 (3 vol.%) at 10 °C min^{-1}. The locations of subsequent isothermal experiments are identified by vertical dotted lines.

RESULTS OF EXPLORATORY TANGENTS

Isothermal serpentine

- The extent of dehydration of serpentine is greater while isothermally holding at associated temperatures than while ramping through them.
- The plateau of mass loss suggests an additional ~1 % of mass loss between 605 and 800 °C.

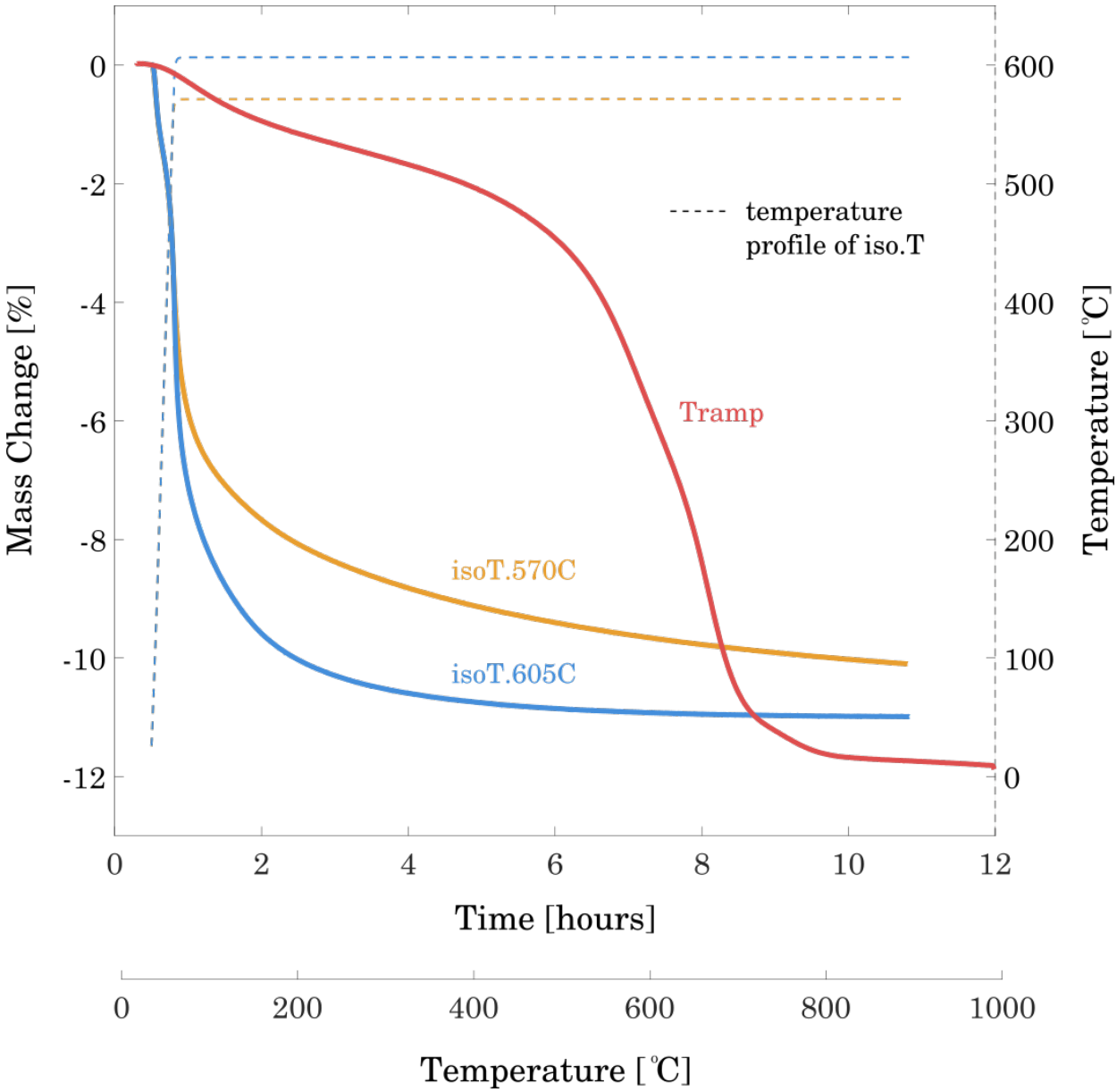

Figure 11. The behaviour of serpentine's mass when ~39 and ~37 mg is heated to 570 (*isoT.570C* in orange) and 605 °C (*isoT.605C* in blue) respectively. The mass loss curve of a temperature ramp of serpentine to 1000 °C is also shown (*Tramp* in red).

- Compared to the ramp HT-PXRD in Figure 7, heightened fosterite peaks (~25° group) in Figure 12 are in agreement with the increased extent of mass loss at 570 °C shown Figure 11.
- Lizardite peak persistance is unexpected when relating the extent of mass loss to HT-PXRD results of Figure 7.

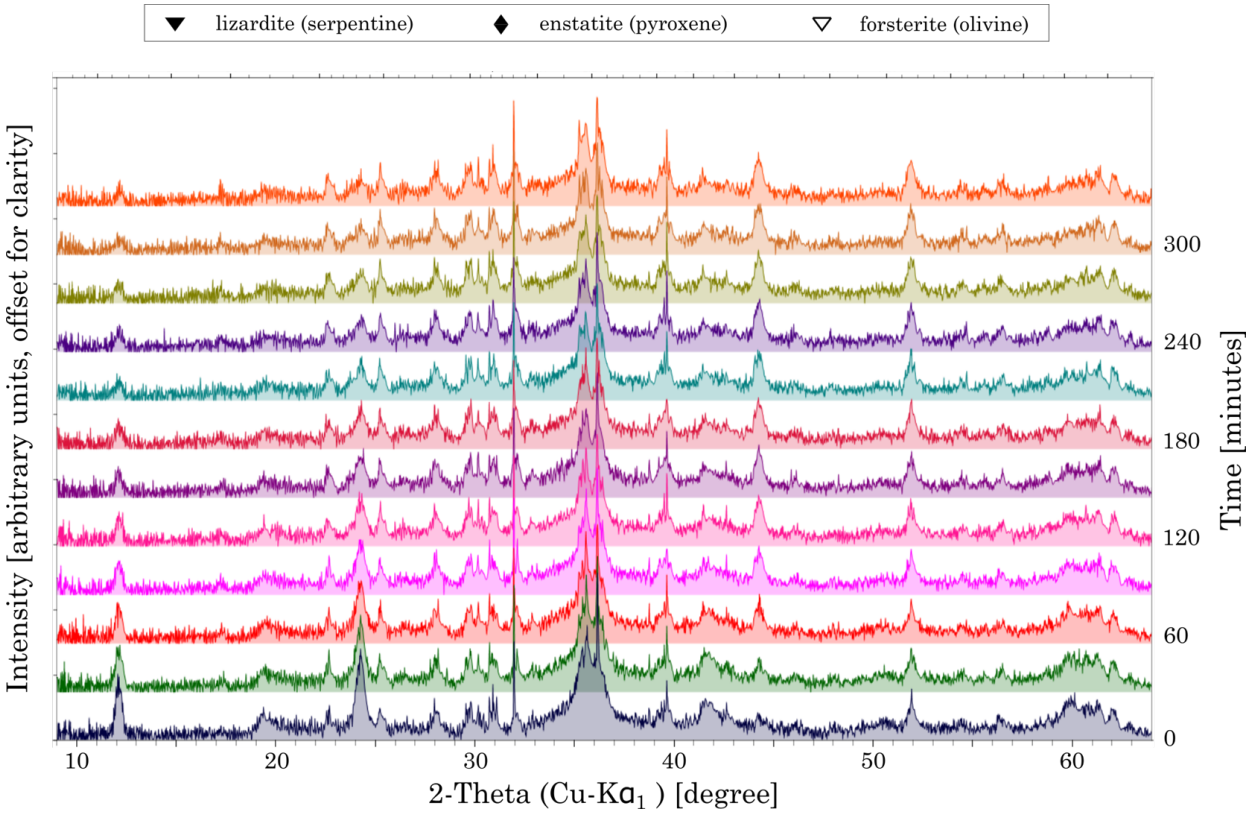

Figure 12. A temporal, isothermal series of ($K\alpha_1$ subtracted) HT-PXRD patterns of as-received serpentine when held at 570 °C for 5 hours.

- At 605 °C, the premature lizardite decomposition (12° and 24° in Figure 13), relative to ramp HT-PXRD, is consistent with the increased extent of mass loss.
- The intermediate mass loss of Figure 11 is consistent with the HT-PXRD suggestion of an equivalent temperature of 675 - 700 °C (right shoulder of the 35.5° peak, and the relative heights between the 35.5° and 35° peaks).

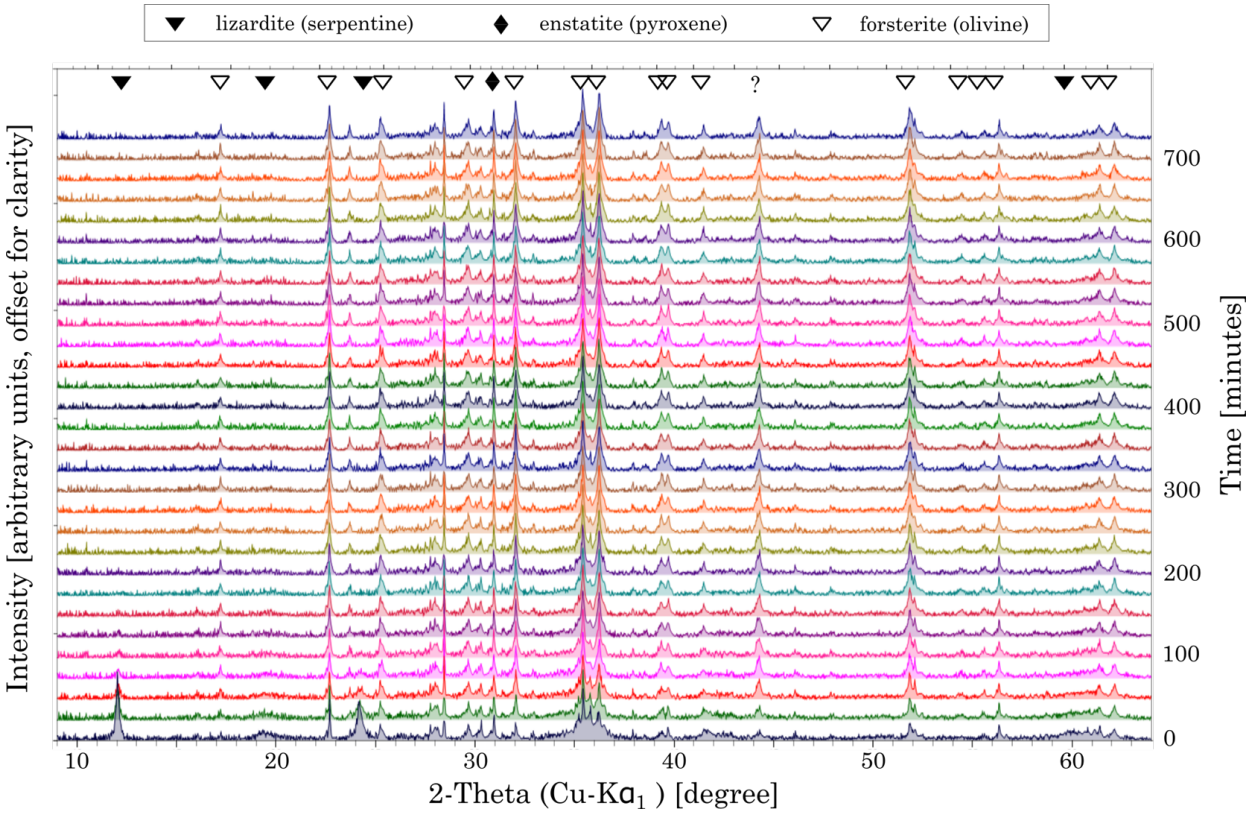

Figure 13. A temporal, isothermal series of ($K\alpha_1$ subtracted) HT-PXRD patterns of as-received serpentine when held at 605 °C for 12 hours.

Graphite mixed serpentine

- Graphite does not seem to signifiactly effect the mass loss of serpentine.

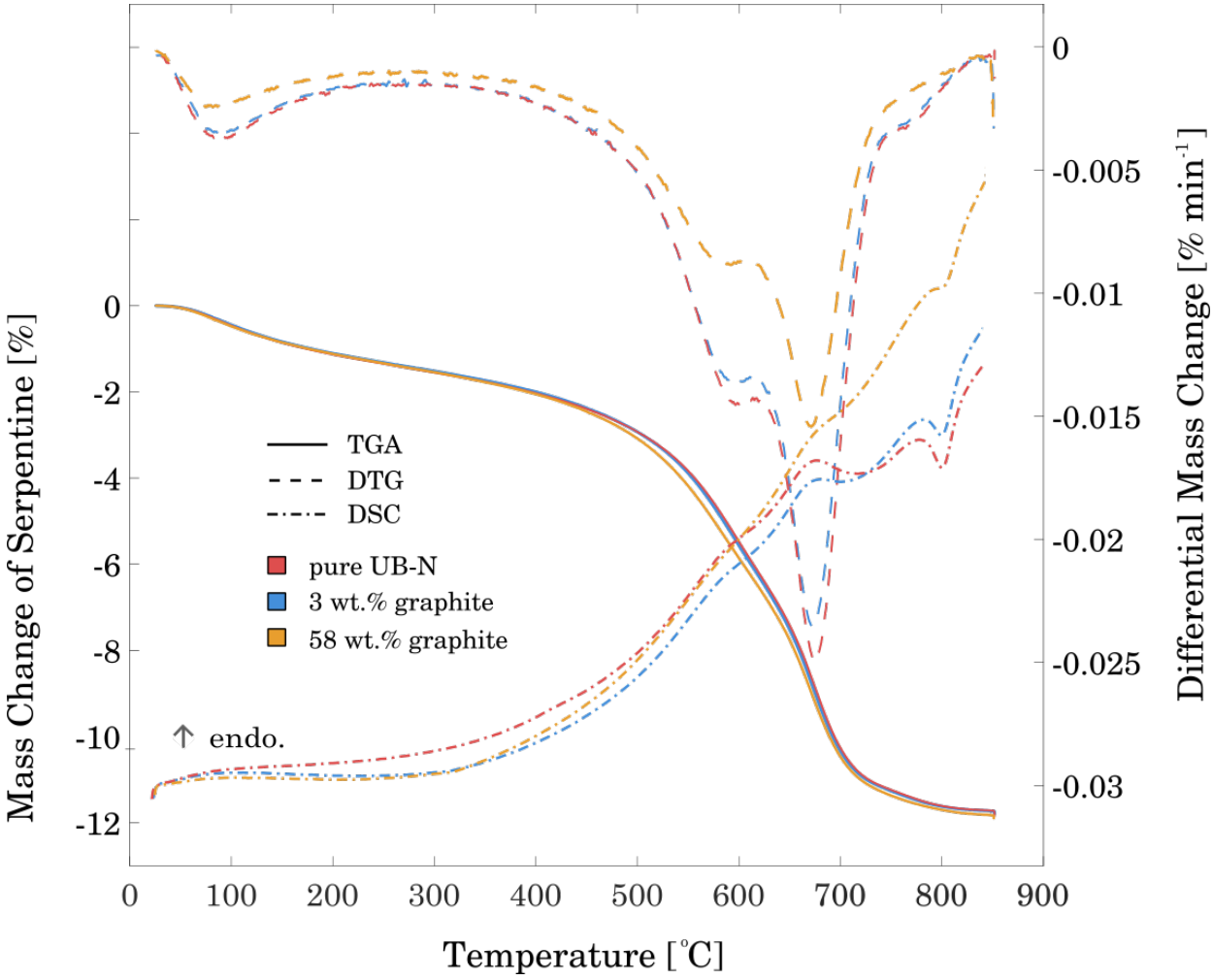

Figure 14. The behaviour of serpentine's mass and thermal energy when ~36 and ~16 mg is heated under the same conditions in the presence of ~3 and ~58.8 wt.% of graphite respectively.

- No effect of graphite's presence is observed on the thermal behaviour of serptine or forsterite's long-range order; peaks degrade and form at the same temperatures and, similarily, a high background forms at intermediate temperatures.

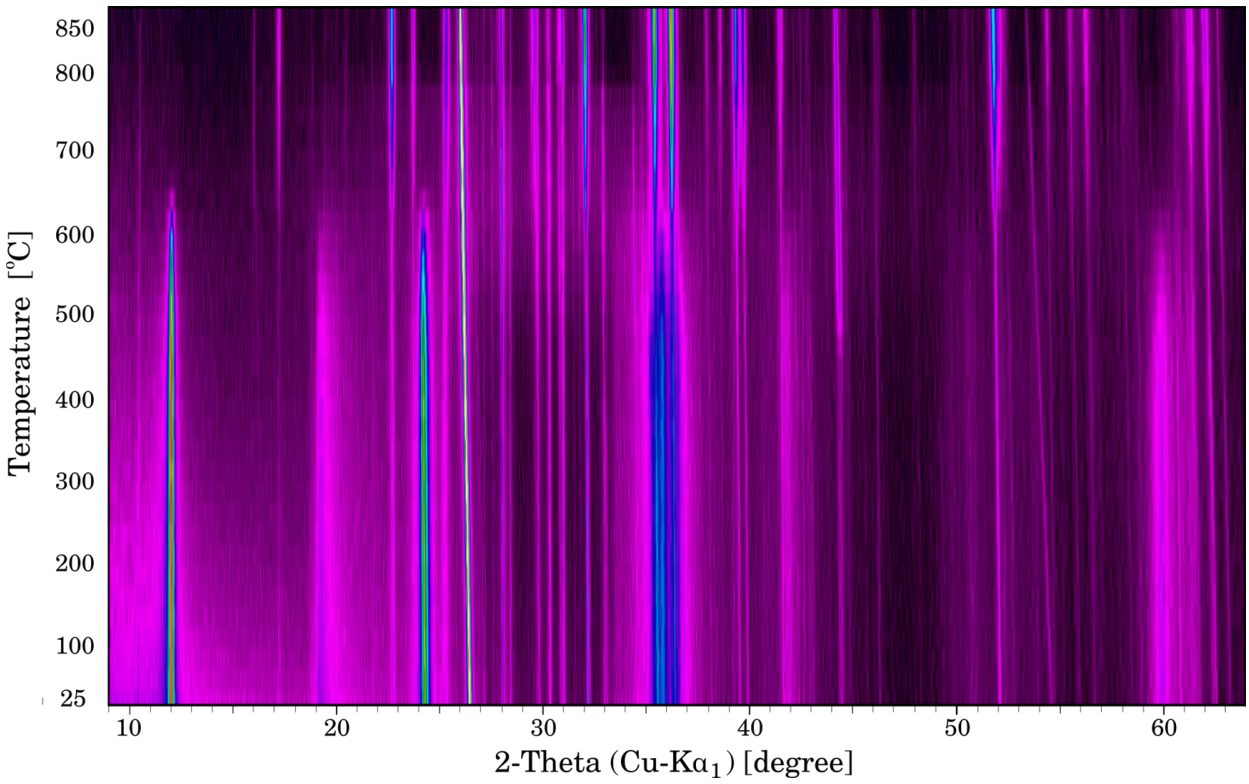

Figure 16. A heat map of the HT-PXRD thermal series of serpentine mixed with ~3 wt.% graphite.

WHERE THIS WORK WILL LEAD

Upon completion of a more thorough study into phyllosilicate's response to heat, we intend to scrutinize our results against the predicted thermal and impact history of NEO's, including Ryugu [4, 5, 9]. In the context of the associated doctoral work, we will apply these eventual results to aid in the interpretation of hyper-velocity impact studies that are planned in the near future. These include using the 2-stage light gas gun of the Centre for Astrophysics and Planetary Science at the University of Kent, and performing pulsed laser shots with the Unité Matériaux et Transformations at the Université de Lille.

Efforts into developing an experimental campaign around femtosecond pulsed laser shots have in fact already begun. As shown in Figures 17 and 18, we will apply surface imaging techniques (e.g profilemetry) to characterize microcrater's physical morphology, electron microscopy to study individual craters, along with spectroscopy in an attempt to have space-mission related results.

[VIDEO] https://www.youtube.com/embed/59Gn5WwXvlM?rel=0&fs=1&modestbranding=1&rel=0&showinfo=0

Figure 17. Topographically reconstructed microcraters generated by a femto-second pulsed laser (1030 nm) on a polished chip of serpentine.

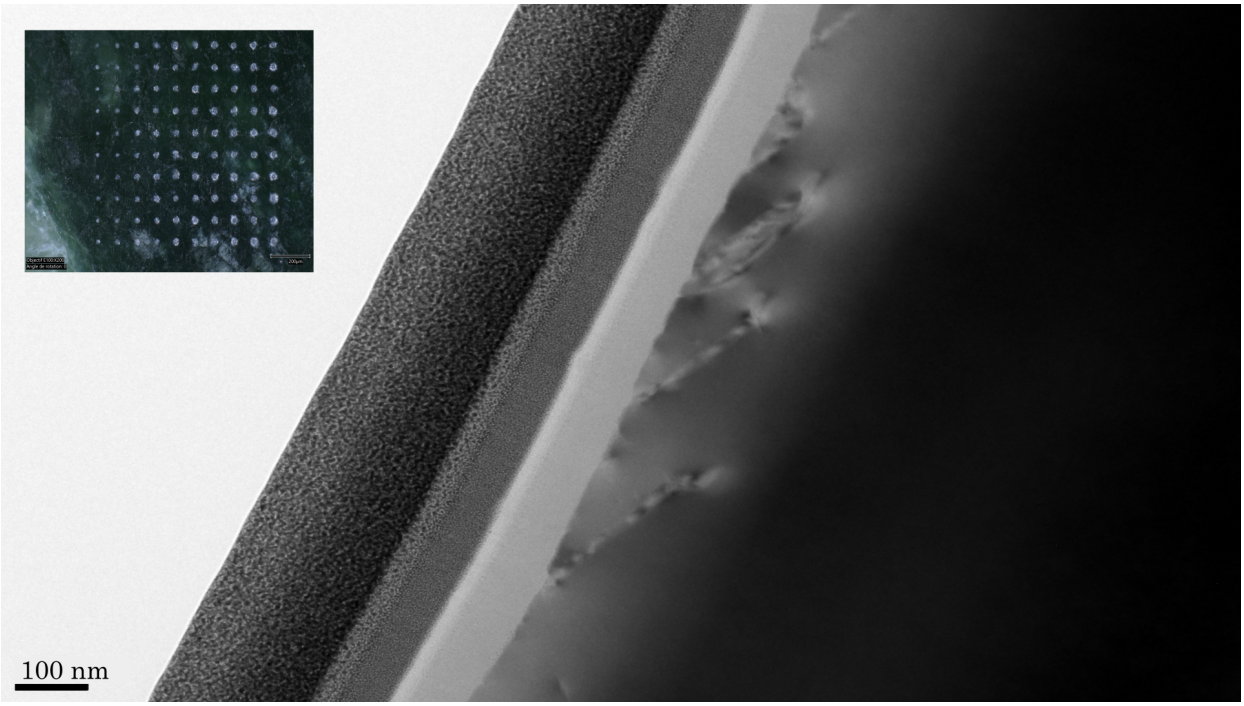

Figure 18. A TEM bright-field image collected on the cross-section of a laser-generated microcrater in a polished chip of San Carlos olivine (extracted by focused ion beam after depositing a protective platinum coating).

Looking forward, we intend to also further this work on phyllosilicate thermal behaviour in the following ways:

- expand our investigation beyond serpentine, to explore the intracies of the role of different cations and atomic structures.
- perform both long(er) isothermal heating and thermal fatigue (cyclic) experiments.
- explore the effect of a vacuum environment.
- explore the amorphous constituents of decomposed serpentine using SEM, TEM, and their associated techniques (EDS, HAADF, ect.).

ACKNOWLEDGEMENTS AND THANKS

The authors thank the Chevreul Institute (FR 2638) at the Université de Lille for access to the XRD (http://uccs.univ-lille1.fr/index.php/fr/ressources/2-non-categorise/59-diffraction-x) and electron microscopy (https://pmel.univ-lille.fr/nc/en/?lang=en&cHash=92f7d8469c9aede426446a2fef4e376a) (https://pmel.univ-lille.fr/index.php?lang=fr) platforms, the I-SITE ULNE (Université Lille Nord Europe), and the MEL (Métropole Européenne de Lille). The serpentine UB-N aliquot was procured from the Service d'Analyse des Roches et des Minéraux (SARM (http://sarm.cnrs.fr/index.html)) in Nancy, France. The authors also thank L. Burylo and N. Dielal, from the Université de Lille, for their help performing the XRD and STA respectively. David Troadec, of the Institut d'Électronique, de Microélectronique et de Nanotechnologie (IEMN (https://www.iemn.fr)) - UMR 8520, is acknowlegded for extracting samples by focused ion beam milling for the TEM image. Tom Blanton and Rongsheng Zhou of the ICDD are appreciated for their advice regarding their MDI-JADE (https://www.icdd.com/mdi-jade/?gclid=Cj0KCQiA7YyCBhD_ARIsALkj54pFOwkDKBJpVCLWLNsf1CZ_5ORA43UNGoVow-yG1BPb7PKcp94NGY0aAgwKEALw_wcB) software, and the modifications made to JADE from our feedback. Lastly, the relentless efforts of Emmanuel Dubois, and Flavie Braud in particular, are greatly appreciated in the initial laser-shot experiments, performed at the Laser procEssing plAtform for multiFunctional electronics (https://leaf-equipex.iemn.univ-lille1.fr) at the IEMN, Université de Lille.

AUTHOR INFORMATION

Dan Hallatt is a doctoral candidate in a cotutelle PhD agreement between the Unité Matériaux et Transformations at the Université de Lille, France (supervised by Hugues Leroux) and the Centre for Astrophysis and Planetary Science at the University of Kent, UK (supervised by Mark Burchell and Penny Wozniakiewicz).

REFERENCES

[1] Hamilton V. E. et al. (2019) Nat. Astron., 3, 332-340. (https://www.nature.com/articles/s41550-019-0722-2)

[2] Kitazato K. et al. (2019) Science., 364, 272-275. (https://science.sciencemag.org/content/364/6437/272.abstract)

[3] Le Guillou C. et al. (2014) Geochim. Cosmochim. Acta 131, 368–392. (https://www.sciencedirect.com/science/article/abs/pii/S0016703713006595)

[4] Morota T. et al. (2020) Science, 368, 654-659. (https://science.sciencemag.org/content/368/6491/654)

[5] Kitazato K. et al. (2021) Nat. Astron., doi/.org/10.1038/s41550-020-01271-2 (https://www.nature.com/articles/s41550-020-01271-2?utm_source=other&utm_medium=other&utm_content=null&utm_campaign=JRCN_1_DD01_CN_NatureRJ_article_paid_XMOL).

[6] Rubino, S. et al. (2020), Planet Sci. J.l, 1, 61. (https://hal.univ-lille.fr/hal-03134243/document)

[7] Gayk, T., & Kleinschrodt, R. 2000, JMetG, 18, 293. (https://onlinelibrary.wiley.com/doi/10.1046/j.1525-1314.2000.00256.x)

[8] Pohl L. (2020) University of Central Florida-Doctoral Thesis, 269. (https://stars.library.ucf.edu/cgi/viewcontent.cgi?article=1268&context=etd2020)

[9] King, A. et al (2021) Geochim. Cosmochim. Acta, 298, 167-190. (https://www.sciencedirect.com/science/article/abs/pii/S0016703721000971)